

Performance of WO_x -added Mo–V–Te–Nb–O catalysts in the partial oxidation of propane to acrylic acid

Bu Young Jo, Sang Seop Kum, Sang Heup Moon *

School of Chemical & Biological Engineering and Institute of Chemical Processes, Seoul National University, Seoul 151-744, Republic of Korea

ARTICLE INFO

Article history:

Received 5 October 2009

Received in revised form 20 January 2010

Accepted 1 February 2010

Available online 6 February 2010

Keywords:

Propane
Oxidation
Acrylic acid
Tungsten oxide
Dehydration
Acidity

ABSTRACT

The performance of $Mo_{1.0}V_{0.3}Te_{0.23}Nb_{0.23}O_x$ catalyst in the partial oxidation of propane to acrylic acid was improved when the catalyst was modified with an optimal amount of tungsten oxide (WO_x), which was present largely in an amorphous phase. The added WO_x increased the catalyst activity by promoting the dehydration of the oxygenate intermediates in the oxidation process, which eventually accelerated the production of propylene. An increase in the dehydration rates on the W-added catalysts was verified by separate experiments using 1- and 2-propanol as the reactants. The selectivity for the production of acrylic acid was also improved for the W-added catalysts because the dehydration step was promoted to a greater extent than the dehydrogenation step and the number of acidic sites in the catalysts was decreased. The reaction results obtained using the W-added catalysts can be explained based on the reaction paths involved in the propane-oxidation process and on the surface properties of the catalysts analyzed using X-ray diffraction (XRD), infrared (IR) spectroscopy, and the temperature-programmed desorption of ammonia (NH_3 -TPD).

© 2010 Elsevier B.V. All rights reserved.

1. Introduction

Acrylic acid, which is a raw material for synthesizing acrylate polymers for use as plastics, adhesives and paints, is commercially produced by the partial oxidation of propylene [1,2]. However, an alternative process is under investigation to produce acrylic acid directly from propane, which is cheaper than propylene. A key to the success of the new process is a catalyst that effectively activates the relatively stable propane and allows the production of acrylic acid at high yields. A few catalysts have been proposed for the purpose, but they still need further improvement prior to commercialization [1,3,4].

The application of multi-component metal oxide (MMO) catalysts for the oxidation of propane to acrylic acid started in the 1990s, although Mo–V–Nb mixed oxide that formed the basis of the catalysts was proposed for the oxidation of ethane to ethene and acetic acid in the 1970s [5]. The Mo–V–Nb oxide catalyst also activated propane at 300 °C but the products were only acetic acid, acetaldehyde and carbon oxides. Also studied was Mo–V–Te oxide catalyst, which achieved high propane conversions but again produced no acrylic acid. Although mixed oxide catalysts lacking V

were very active for propylene oxidation [6–8], they were not so active for propane oxidation [9,10].

The most effective catalysts for propane oxidation to acrylic acid were Mo–V–Te–Nb–O types reported by Ushikubo et al. [3] and Lin and Linsen [11], who observed significantly higher activities of the above catalysts compared with the cases of other ones. The catalyst performance could be further improved by substituting Te of Mo–V–Te–Nb–O with Sb [12]. A similar study was made independently by Takahashi et al. [13]. However, the yields of acrylic acid obtained using these catalysts were reported to remain below 48% [1], which makes the propane-oxidation process still less competitive with the current process based on propylene oxidation.

Because the rate-determining step (RDS) of propane oxidation is the formation of propylene from propane, one of strategies to improve the catalyst is to promote it with a proper component that is expected to accelerate the conversion of propane to propylene. Propylene is obtained as an intermediate in propane oxidation either by a single step, the oxidative dehydrogenation of propane, or by two steps that involve the initial oxidation of propane to 1- or 2-propanol and the subsequent dehydration of propanol to propylene [12,14,15].

According to a previous report, VO_x/Al_2O_3 promoted with amorphous tungsten oxide (WO_x) shows an improved activity for the oxidative dehydrogenation of propane to propylene [16]. WO_x is reported to be an active catalyst for the dehydration of alcohols

* Corresponding author. Tel.: +82 2 880 7409; fax: +82 2 875 6697.
E-mail address: shmoon@surf.snu.ac.kr (S.H. Moon).

such as methanol and 2-propanol [17,18]. In this study, we attempted to increase the activity of Mo–V–Te–Nb oxide, a known catalyst for the partial oxidation of propane to acrylic acid [19–21], by promoting it with different amounts of WO_x .

The prepared catalysts were tested for propane oxidation and also for the oxidation of 1- and 2-propanol. The latter compounds were used as the model reactants because they were obtained as the intermediates of propane oxidation. The reaction results were correlated with the surface properties of the catalysts, which were analyzed by X-ray diffraction (XRD), infrared spectroscopy (IR), and the temperature-programmed desorption of ammonia (NH_3 -TPD).

2. Experimental

2.1. Catalyst preparation

A model catalyst with the nominal composition of Mo/V/Te/Nb = 1.0/0.3/0.23/0.23, based on the amounts of the individual components that were added to the preparation solution, was prepared by a co-precipitation method [14,19–21]. The precursors of metal oxides were hexaammonium heptamolybdate tetrahydrate ($(NH_4)_6Mo_7O_{24} \cdot 4H_2O$), ammonium metavanadate (NH_4VO_3), telluric acid (H_2TeO_6), and ammonium niobate oxalate hydrate ($C_4H_4NNbO_9 \cdot xH_2O$).

For catalyst preparation, 1.18 g of the Mo precursor, 0.23 g of the V precursor and 0.35 g of the Te precursor were diluted in 50 cm³ of distilled water maintained at 35 °C. Another solution was prepared by dissolving 0.24 g of the Nb precursor in 4 cm³ of distilled water. Two solutions were mixed and stirred at 300 rpm in a round flask at 35 °C for 3 h. Nitric acid was added to the mixed solution to control the pH to 3.1 and the resulting solution was stirred for another 1 h. The solution was dried in a rotary evaporator at 70 mbar and 60 °C for 50 min, and additionally dried in an air-circulating oven at 120 °C overnight. Dried catalyst was ground in a pulverizer (Retsch, MM 301) shaking at 20 Hz for 2 min. The catalyst was heated to 200 °C in air at a ramping rate of 4 °C/min and finally calcined in N_2 at 600 °C for 2 h, prior to impregnation with WO_x .

The precursor of W, ammonium tungstate pentahydrate ($(NH_4)_{10}W_{12}O_{41} \cdot 5H_2O$), was added to the model catalyst in different amounts, 0.0005–0.4 wt% based on W metal, by an impregnation method. The prepared catalysts were dried at 80 °C for 1 h and subsequently at 120 °C overnight in an air-circulating oven before they were ground into powders. The powder catalyst was calcined in N_2 while the temperature was raised from 20 to 500 °C at a rate of 5 °C/min and finally maintained at 500 °C for 2 h.

2.2. Reaction

2.2.1. Propane oxidation

Reaction tests were made in a stainless-steel tubular reactor ($ID = 4.5$ mm) at temperatures between 350 and 400 °C using a reactant stream containing propane, oxygen, nitrogen, and water in the molar fractions of 0.08, 0.21, 0.33, and 0.38. The catalysts used in the reaction were powders of 180–250 μm in size, which were obtained by meshing. Diluent of the catalyst was not used. The reactor contained 0.1 g of the catalyst, and the space velocity of the reactant stream was 1000 h⁻¹. A gas line connecting the reactor with a gas chromatograph was maintained at 180 °C to prevent the products from possible condensation or polymerization during flow in the line. The gas chromatograph (GC) was equipped with a flame ionization detector (FID) for analyzing hydrocarbons and a thermal conductivity detector (TCD) for analyzing nitrogen, oxygen, and carbon oxides. Two parallel capillary columns, CP- Al_2O_3/KCl (Varian) and SOLGEL WAX (SGE), were used for the

separation of hydrocarbons, and a 60/80 CARBOXEN 1000 (Supelco) column for the separation of nitrogen, oxygen, CO and CO_2 . The conversion of propane was calculated based on carbon balance and the selectivity for acrylic acid from the amounts of produced acrylic acid compared with those of converted propane.

2.2.2. 1- or 2-propanol oxidation

The oxidation of 1- or 2-propanol was carried out at 200 or 175 °C using a reactant stream containing 1-propanol (or 2-propanol), oxygen, nitrogen, and water in the molar fractions of 0.08, 0.21, 0.33, and 0.38, respectively. The reason for carrying out propanol oxidation at lower temperatures than in the case of propane oxidation was because propanol oxidation proceeded very rapidly at 350–400 °C such that differences in the rates among sample catalysts could not be observed. The amounts of the catalyst and the space velocity of the reactant stream were the same as for propane oxidation.

2.3. Catalyst characterization

2.3.1. XRD and ICP-AES

The catalysts were analyzed by X-ray diffraction (XRD: MAC Science Co., M18XHF-SRA). The crystalline phases of the catalyst components were identified based on the XRD-peak assignments made in a previous study [22]. The amounts of metal species in the catalyst were estimated by inductively coupled plasma-atomic emission spectroscopy (ICP-AES: Perkin-Elmer (USA), Optima 4300DV).

2.3.2. FT-IR and NH_3 -TPD

The infrared (IR) spectra of the catalysts were recorded on an FT-IR (Midac, model M2000) instrument, which was equipped with an MCT detector and a diffuse reflectance accessory (Pike Technologies Inc., DiffusIR Accessory). As the catalyst powders were weighed in the same amount, 0.07 g, and placed in the DRS cell of a fixed dimension, 5 mm \times 5 mm \times 5 mm, the IR peaks were obtained with reproducible intensity. The amounts of acidic sites on the catalyst surface were estimated from the results of the temperature-programmed desorption of ammonia (NH_3 -TPD) obtained using a catalyst analyzer (Bel-Cat, Bel Japan Inc.). For the NH_3 -TPD, the catalysts were pre-treated in He at 110 °C for 1 h and then cooled to 20 °C, prior to adsorption with NH_3 at atmospheric pressure. After purging the reactor with He at room temperature for 1 h, NH_3 -TPD peaks were recorded while the temperature was raised from 20 to 650 °C at a rate of 10 °C/min. The effluent gas was analyzed for NH_3 with a TCD.

2.3.3. O_2 -TPD

The oxygen mobilities of the catalysts were evaluated based on the results of the temperature-programmed desorption of oxygen (O_2 -TPD) obtained using a TCD. For the O_2 -TPD, the catalysts were pre-treated in argon at 150 °C for 1 h and then cooled to 20 °C prior to the desorption of O_2 at atmospheric pressure. The same amount of the sample catalysts, 0.1 g, was used for the experiments. O_2 -TPD peaks were recorded while the temperature was raised from 20 to 650 °C at a rate of 10 °C/min. The effluent gas was analyzed for O_2 with a TCD.

3. Results

3.1. Composition and crystallinity of prepared catalysts

The ICP-AES results indicated that the model catalyst, which was prepared with a nominal composition of Mo/V/Te/Nb = 1.0/0.3/0.23/0.23, contained individual components with atomic ratios of Mo/V/Te/Nb = 1.0/0.26/0.21/0.24, which were not affected by

Table 1

The W contents and surface areas of the sample catalysts.

W loading (wt%)	W/Mo ($\times 10^3$) ^a	W/Mo ($\times 10^3$) ^b	Surface area ^c (m ² /g)
0.01	0.3	0.3	5.3
0.02	0.5	0.7	5.1
0.05	1.3	1.1	5.3
0.1	2.6	2.3	5.2
0.2	5.1	4.6	5.2
0.4	10.6	9.2	5.3

^a The nominal atomic ratios of W to Mo used in the preparation step.^b The atomic ratios of W to Mo measured by ICP-AES.^c Surface area of model catalyst: 5.2 m²/g.

the W addition. The atomic ratios of W to Mo in the prepared catalysts were lower than the nominal ratios used in the preparation step, but the two sets of values changed in parallel with each other, as shown in Table 1. The W/Mo ratios for the catalysts containing W in the amounts lower than 0.005 wt% were not obtained because the W amounts were below the detection limit of ICP-AES. According to the XRD patterns shown in Fig. 1, the model catalyst contained the crystallite phases of Mo_{5-x}(V/Nb)_xO₁₄ ($2\theta = 22.1^\circ, 23.3^\circ, 25.2^\circ, 29.7^\circ, 31.5^\circ, 32.4^\circ$ and 33.5°), TeM₃O₁₀ ($2\theta = 22.1^\circ, 28.2^\circ, 36.2^\circ, 45.2^\circ$ and 50.0°), and Te₂M₂₀O₅₇ ($2\theta = 22.1^\circ, 26.2^\circ, 26.8^\circ, 27.3^\circ, 29.2^\circ$, and 35.4°), where M in the equations represented either Mo, V or Nb [22–24].

The XRD result remained the same and the peaks representing the crystalline phase of WO₃ were not observed in the W-added catalysts, probably because the amounts of added W were small, with W/Mo ratios less than 0.01.

3.2. Propane oxidation

Fig. 2 shows changes in the conversion of propane obtained at different reaction temperatures with the amounts of added W, which are presented in a log scale to cover the wide range of the W amounts. The conversions were enhanced by the W addition and showed a maximum when the W/Mo ratio was between 2.6×10^{-4} and 5.1×10^{-4} for all reaction temperatures.

The selectivity for acrylic acid decreased with an increase in the conversion, as shown in Fig. 3a, because acrylic acid was obtained as an intermediate in the consecutive oxidation of propane that eventually led to the products of higher oxidation. When W was added to the catalyst, the selectivity–conversion curves moved upward, indicating an increase in the selectivity at the same conversion. Similar to the conversions shown in Fig. 2, the selectivity was at the maximum when the W loading was in the

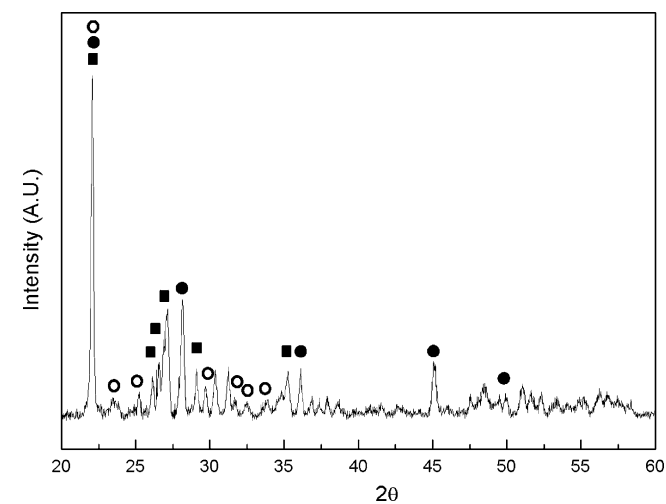


Fig. 1. Crystallite phases of the model catalyst: (○) Mo_{5-x}(V/Nb)_xO₁₄, (●) Te₁M₃O₁₀ and (■) Te₂M₂₀O₅₇ (M = Mo, V, Nb).

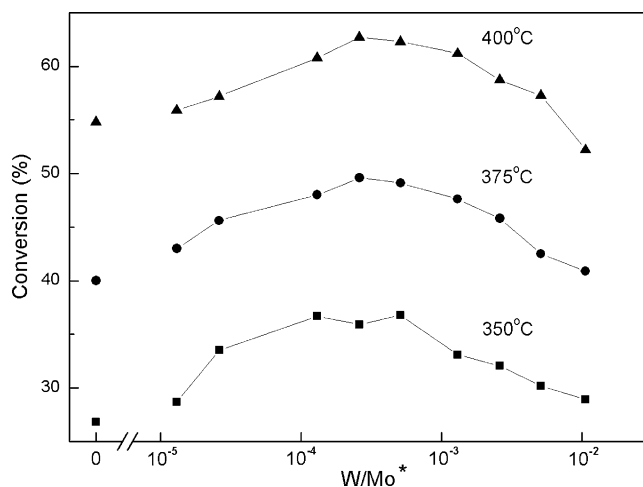


Fig. 2. Performance of sample catalysts in propane oxidation. Reaction condition: catalyst = 0.1 g, temperature = 350–400 °C, propane:oxygen:nitrogen:water = 0.08:0.21:0.33:0.38 (molar fractions). *The nominal atomic ratios of W to Mo used in the preparation step.

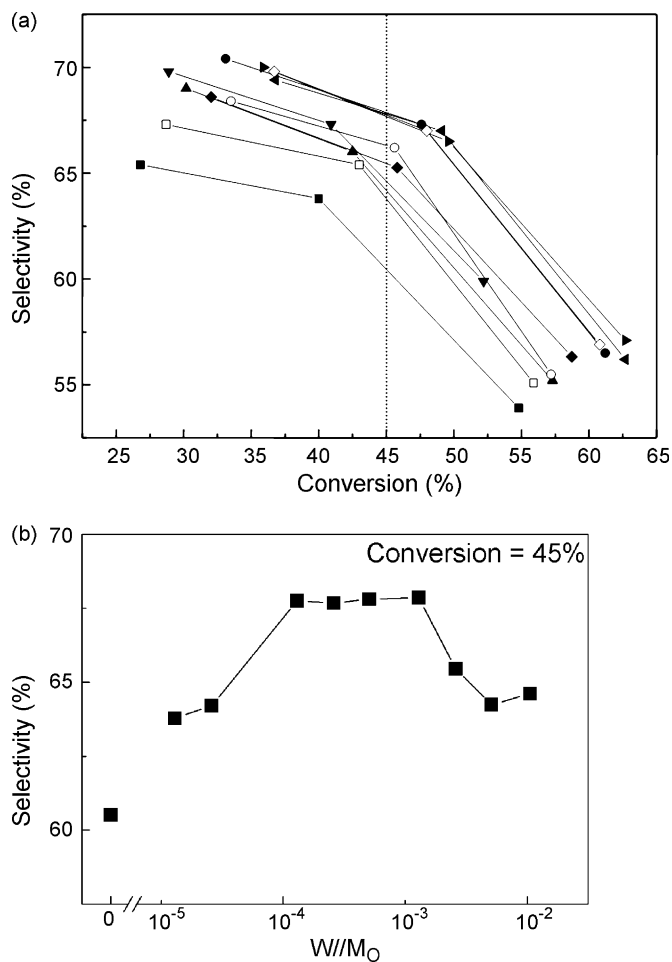


Fig. 3. (a) Changes in the selectivity for the production of acrylic acid in propane oxidation. The nominal W/Mo ratios used in the preparation step: (■) 0, (□) 1.3×10^{-5} , (○) 2.6×10^{-5} , (◇) 1.3×10^{-4} , (▶) 2.6×10^{-4} , (◀) 5.1×10^{-4} , (●) 1.3×10^{-3} , (◆) 2.6×10^{-3} , (▲) 5.1×10^{-3} and (▼) 1.1×10^{-2} . (b) The acrylic-acid selectivity obtained at a fixed 45% conversion versus the W/Mo ratio.

proper range, as demonstrated in Fig. 3b in the case of a 45% conversion. The selectivity increased with an initial increase in the W/Mo ratio up to about 1.3×10^{-4} and remained constant until it started to drop at ratios higher than 1.3×10^{-3} .

Table 2
Product distribution in propane oxidation at a fixed conversion, 45%.

W/Mo ($\times 10^3$)	Products (%) (propane conversion = 45%)					
	Acrylic acid	Propylene	Acetic acid	Acetone	CO	CO ₂
Model catalyst	60.5	4.9	4.2	0.34	16.3	13.8
0.013	63.8	5.3	4.5	0.21	13.9	12.3
0.026	64.2	5.2	4.8	0.13	14.0	11.7
0.13	67.7	6.5	5.3	0.19	10.8	9.5
0.26	67.6	6.9	5.1	0.16	11.4	8.8
0.51	67.8	6.7	5.2	0.12	10.9	9.3
1.3	67.9	6.4	5.2	0.14	11.3	9.1
2.6	65.5	6.1	4.8	0.20	12.9	10.5
5.1	64.2	5.6	4.3	0.17	14.3	11.4
10.6	64.6	5.5	4.6	0.25	13.8	11.2

The product distribution in propane oxidation is provided in Table 2. The fractional amounts of propylene and acetic acid change with the W/Mo ratio, showing a similar trend as in the case of acrylic acid, while the amounts of CO and CO₂ show an opposite trend. The amounts of acetone are insignificant compared with the other products.

3.3. Oxidation of 1- or 2-propanol

As mentioned above, propylene is produced either by a single step, the oxidative dehydrogenation of propane, or by two steps that consist of the initial oxidation of propane to propanols and the subsequent dehydration of the propanols. In this study, we tested the W-added catalysts for the conversion of propanols.

Fig. 4 shows the conversions and the amounts of three major products obtained in 1-propanol oxidation carried out at 200 °C using the W-added catalysts. According to previous studies [12,14,15], 1-propanol is converted via two routes: the dehydrogenation of 1-propanol to produce propionaldehyde, which is further oxidized to propionic acid, and the dehydration of 1-propanol to produce propylene, which is further oxidized to acetone, acetic acid, acrolein, and acrylic acid [12,14,15]. In the present study, propionic acid, propylene, and acetone were obtained as the major products. Propionaldehyde and carbon oxides were also produced but their amounts were small, changing in less than 1% for different catalysts. The reason why neither acrolein nor acrylic acid was observed in this study was because the reaction temperature, 200 °C, was too low to allow further oxidation of propylene to the products.

Fig. 4 illustrates how the conversion of 1-propanol significantly increased with an increase in the W/Mo ratios up to about

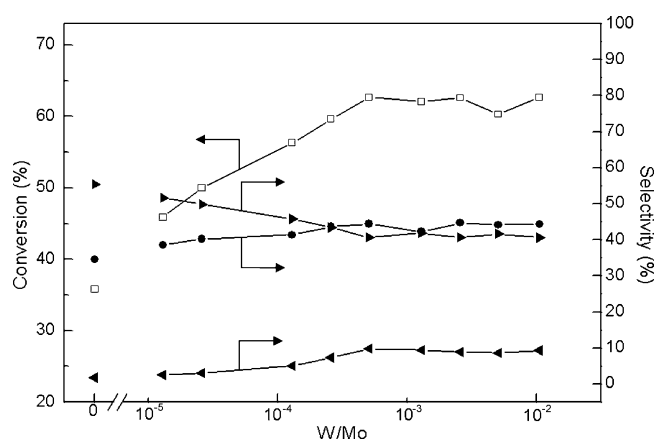


Fig. 4. Performance of sample catalysts in 1-propanol oxidation: (□) conversion of 1-propanol, (▴) selectivity for the production of propionic acid, (●) selectivity for the production of propylene and (▾) selectivity for the production of acetone.

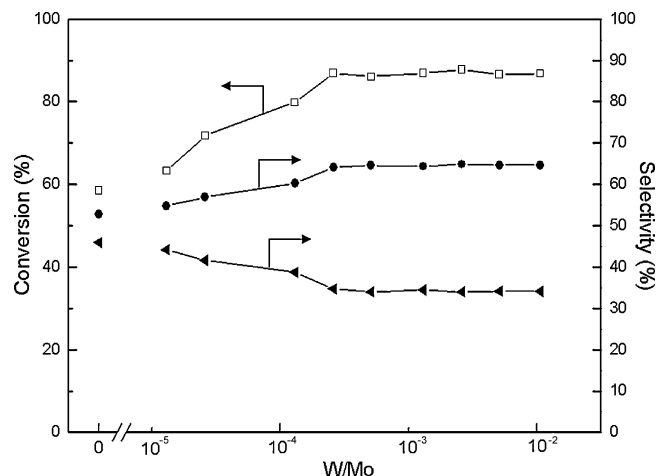


Fig. 5. Performance of sample catalysts in 2-propanol oxidation: (□) conversion of 2-propanol, (●) selectivity for the production of propylene and (▾) selectivity for the production of acetone.

5.1×10^{-4} and leveled off at higher W loading. Similar to the case of the conversion, the selectivities for the production of propylene and acetone also increased with an increase in the W/Mo ratios up to 5.1×10^{-4} and leveled off, or slightly decreased, at higher loading. On the other hand, the selectivity for propionic acid showed a trend nearly opposite that of propylene. The above results indicate that the enhanced catalytic activities of the W-added catalysts for 1-propanol oxidation were obtained largely because the dehydration step, instead of the dehydrogenation step, was promoted by the W addition.

The added W species also promoted the catalytic activity for the oxidation of 2-propanol, as shown in Fig. 5. Among two major products of the process, propylene was produced in increased amounts nearly in parallel with the amounts of added WO_x up to the W/Mo ratios of 2.6×10^{-4} and reached a saturation level at higher W loading. On the other hand, acetone was produced showing a trend nearly opposite to that of propylene. In 2-propanol oxidation, propylene is produced by the dehydration of 2-propanol, similar to the case of 1-propanol oxidation, but acetone is produced by the direct dehydrogenation of 2-propanol, unlike the case of 1-propanol oxidation. Carbon oxides were obtained in small amounts similar to the case of 1-propanol oxidation. Accordingly, the results of Fig. 5 indicate the same effect of added WO_x as for 1-propanol oxidation: the promotion of the dehydration step instead of the dehydrogenation step.

3.4. Catalyst characterization

Fig. 6a shows the IR spectra of the catalysts containing different amounts of added W. Peaks appearing in the 900–1000 cm⁻¹ range (Region I) are assigned to the symmetric stretching vibration of Mo=O and those in the 700–900 cm⁻¹ (Region II) range to the asymmetric vibration of Mo–O–M (M = Mo, Te, Nb) [24]. A new peak observed at 975 cm⁻¹ in the W-added catalysts is ascribed to the stretching vibration of W=O in the amorphous phase of WO_x [22,25,26]. As the peak at 845 cm⁻¹, representing the crystalline phase of WO₃ [25], was observed at low intensities for all catalysts, it can be concluded that the added W species were present largely as an amorphous phase instead of a crystalline one, at least when the W/Mo ratio was lower than about 2.6×10^{-4} . The amounts of amorphous WO_x, represented by a peak at 975 cm⁻¹, increased and eventually leveled off with an increase in the W loading, as shown in Fig. 6b.

Fig. 7 shows that the amounts of the acidic sites, which were estimated from the intensity of the NH₃-TPD peak, monotonically

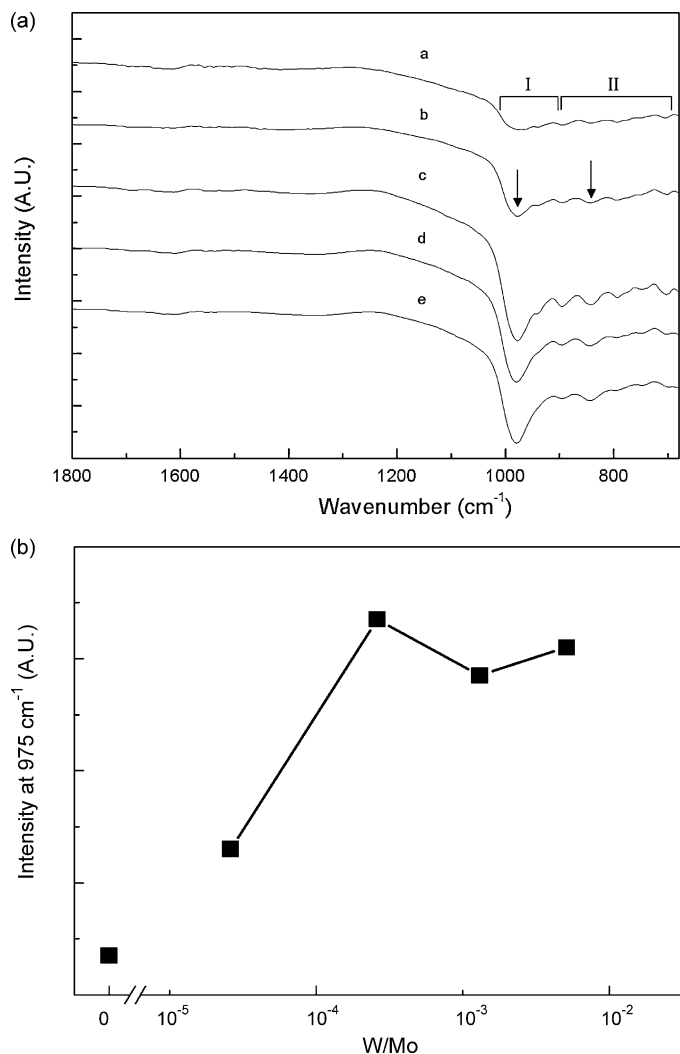


Fig. 6. (a) IR spectra of the catalysts: (a) model catalyst, (b) W 2.6×10^{-5} , (c) W 2.6×10^{-4} , (d) W 1.3×10^{-3} and (e) W 5.1×10^{-3} . *W 2.6×10^{-5} denotes the catalyst modified with W at a nominal W/Mo ratio of 2.6×10^{-5} . (b) Changes in the intensity of IR peak at 975 cm^{-1} with the W/Mo ratios of catalysts.

decreased with an increase in the W loading. The observed trend was not attributed to a decrease in the catalyst surface area, which in fact remained nearly constant in the range of the W loading used in this study.

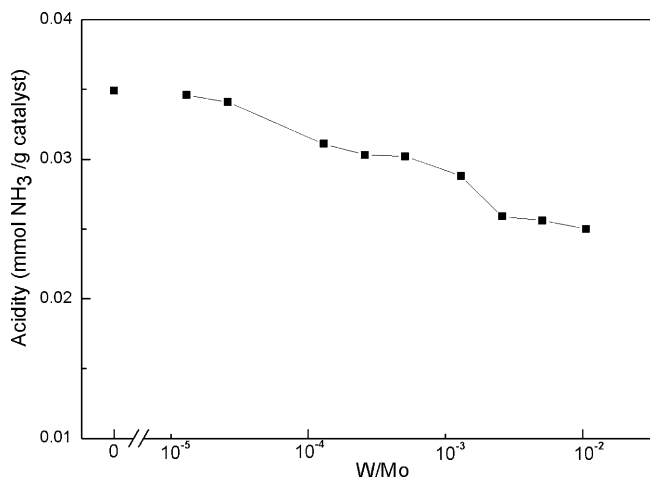


Fig. 7. Changes in the acidity of the catalyst with the W/Mo ratios of catalysts.

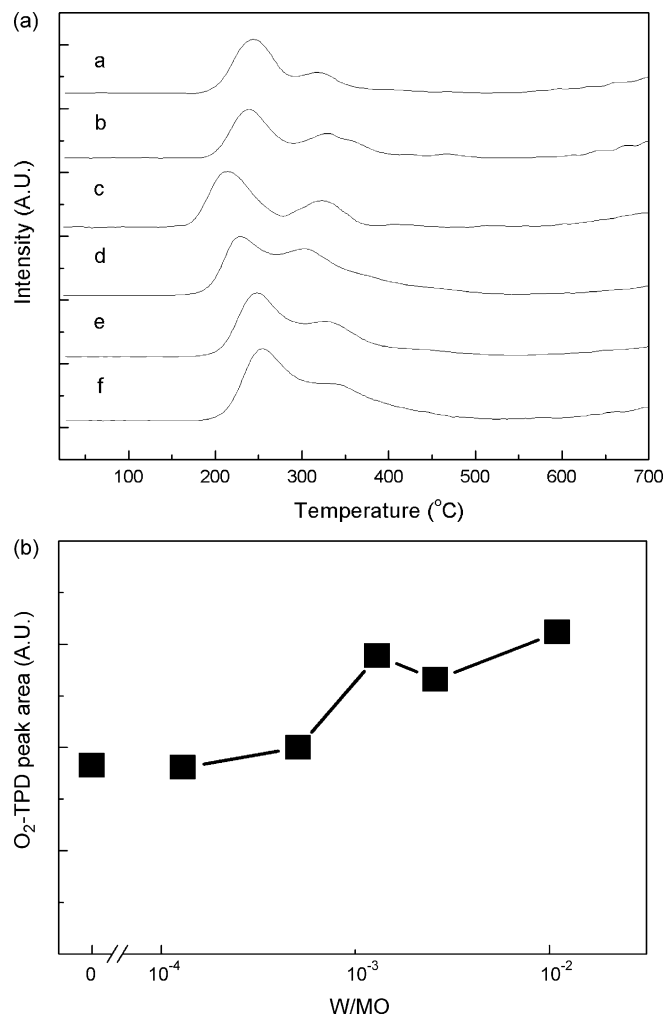


Fig. 8. (a) O₂-TPD from sample catalysts: (a) model catalyst, (b) W 1.3×10^{-4} , (c) W 5.1×10^{-4} , (d) W 1.3×10^{-3} , (e) W 2.6×10^{-3} and (f) W 1.1×10^{-2} . (b) Changes in the amounts of desorbed O₂, represented by TPD-peak areas, with the W/Mo ratios of catalysts.

As shown in Fig. 8a, two peaks were observed in O₂-TPD, which were shifted to lower temperatures with an increase in the W/Mo ratios up to 5.1×10^{-4} . Similar to the trends observed with the conversion of propane and the selectivity for the production of acrylic acid, the oxygen mobility, which was represented by the shift of the O₂-TPD peaks, increased with an increase in the W/Mo ratios up to 5.1×10^{-4} and decreased at higher ratios. The amounts of the relatively weak lattice oxygen, represented by the TPD-peak areas, increased with the W loading, as shown in the insert of Fig. 8b. The activation energies (E_a) for the desorption of the lattice oxygen in the catalysts, which were estimated from the shifts of the TPD peaks with changes in the heating rates (Fig. 9a and b), were 23 and 17 kcal/mol for the model and W 5.1×10^{-4} catalysts, respectively.

4. Discussions

4.1. Reaction pathways in propane oxidation

Fig. 10 describes reactions involved in the partial oxidation of propane [12,14,15], which can be grouped into three paths. Path I comprises the conversion of propane to propylene, which is further oxidized to acrylic acid via acrolein. Path II involves the oxidation of propane to 1-propanol, which is subsequently converted to

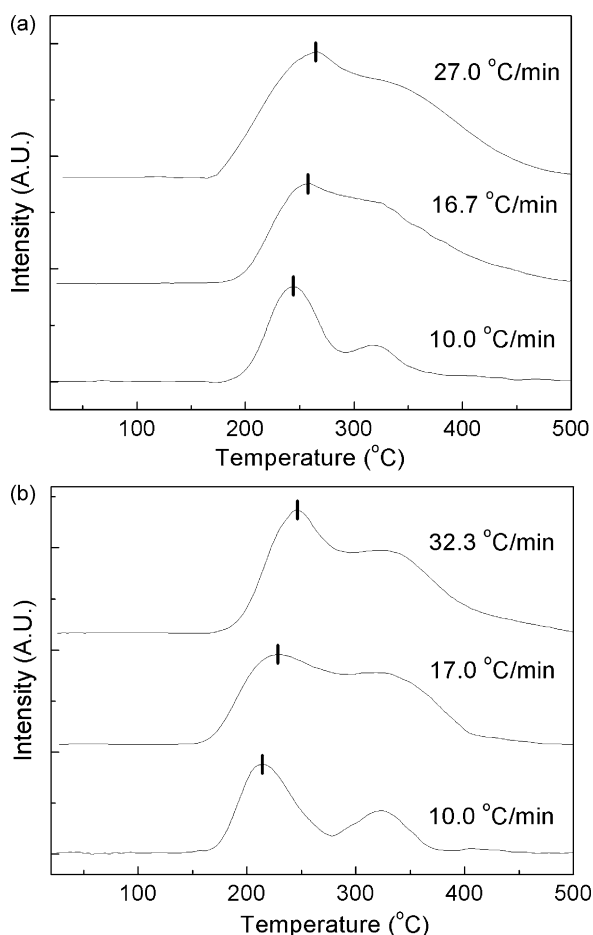


Fig. 9. (a) O₂-TPD from model catalyst obtained at different heating rates. (b) O₂-TPD from W 5.1 × 10⁻⁴ catalyst obtained at different heating rates.

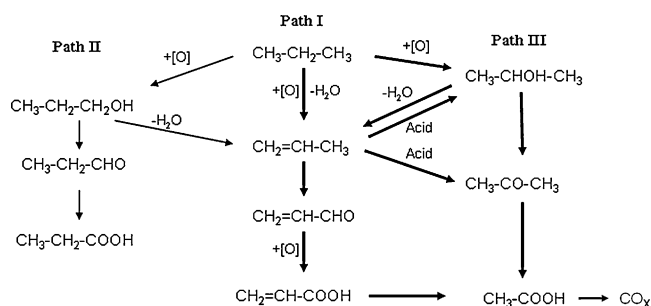


Fig. 10. Reaction pathways in propane oxidation [12,14,15].

propylene by dehydration or to propionaldehyde and propionic acid by further oxidation. Path III is similar to Path II except that propane is oxidized to 2-propanol, which is either dehydrated to propylene or further oxidized to acetone and acetic acid. Additional steps to produce 2-propanol by propylene hydration and acetone by propylene oxidation were also proposed. Between two paths involving propanols, Path II is much slower than Path III and therefore the products of Path II are obtained in smaller amounts [14]. When the process is carried out at high temperatures, the oxygenate products are further oxidized to carbon oxides, thus lowering the selectivity for acrylic acid production.

In Path I, propylene is produced by the oxidative dehydrogenation of propane, which proceeds by the initial oxidation of propane to the oxygenate species on the catalyst surface, followed by the dehydration of the surface oxygenates to propylene. In fact, this mechanism is similar to that of the steps leading to the production

of propylene in Paths II and III, which involve the oxidation of propane to propanols and the subsequent dehydration of the alcohols to propylene. An apparent difference between the two cases is that the reaction intermediates produced in Path I remain on the catalyst as the surface species while those in Paths II and III are desorbed as molecular propanols. Accordingly, it can be suggested from the above consideration that the conversion of propane to propylene, which is the rate-determining step (RDS) of the propane-oxidation process, can be accelerated by the promotion of either or both of the two steps: the partial oxidation of propane to oxygenates, including propanols, and the dehydration of the oxygenates to propylene.

4.2. Oxidation of 1- or 2- propanol

The results of propanol oxidation, shown in Figs. 4 and 5, indicated that the added W species promoted the dehydration step to a greater extent than either the dehydrogenation or the oxidation step and consequently increased the amounts of produced propylene until the W/Mo ratio was about $(2.6\text{--}5.1) \times 10^{-4}$. These results agree with previous reports that amorphous WO_x was active for the dehydration of alcohols [17,18]. The IR observation of the catalysts, shown in Fig. 6a, verified that the added W species were present largely as amorphous WO_x when the W/Mo ratio was lower than about 2.6×10^{-4} . At higher W loading, the propanol conversions remained nearly constant, or slightly decreased, because parts of the added W species were in a crystalline phase, which was inactive for the dehydration and simply covered the catalyst surface.

The selectivity for acetone production increased with the W loading in 1-propanol oxidation but decreased in 2-propanol oxidation. In fact, the opposite trend in acetone production between the two cases is consistent with the fact that the added W species were more active for dehydration than for dehydrogenation. In 1-propanol oxidation, acetone was produced by the oxidation of propylene that had been obtained by the dehydration of 1-propanol. Accordingly, the production of acetone should change in parallel with that of propylene, which was promoted on the W-added catalysts. On the other hand, in 2-propanol oxidation, acetone was produced by the direct dehydrogenation of 2-propanol, which was competing with the dehydration step for a common reactant, 2-propanol. Accordingly, the promotion of the latter step by the W addition would suppress the former step to produce smaller amounts of acetone.

4.3. Activity for propane oxidation

As discussed in Section 4.1, the catalytic activity for propane oxidation can be increased by promoting either or both of the two steps that constitute the RDS of the process: the partial oxidation of propane to oxygenates and the dehydration of the oxygenates to propylene.

Although the promotion of the initial oxidation step leading to oxygenates by the W addition was not confirmed experimentally in the present study, the trend can be anticipated from a previous study that was made with WO_x-added V₂O₅/Al₂O₃ catalysts for the oxidative dehydrogenation of propane [16]. It was reported that the added WO_x species, which themselves were inactive for propane oxidation, increased the activity by providing additional sites for the weak adsorption of propane, which was eventually transferred to, and oxidized on, the V₂O₅ surface.

The significant promotion of the dehydration step in the W-added catalysts was verified in this study by the results of propanol oxidation. Accordingly, the observed increase in the activity of the W-added catalysts can be explained by the fact that the added W

species promoted the two steps involved in the RDS of propane oxidation.

The activity for propane oxidation was also promoted by the increased oxygen mobility in the catalyst [27,28], in addition to the influence of the above-mentioned factors. The O₂-TPD results (Fig. 9a) demonstrated that the activation energy for the desorption of the lattice oxygen was lower for the W-added catalyst than for the unmodified one. This result was obtained because the oxygen mobility increased more in the presence of the structurally random, amorphous WO_x species than in the presence of the crystalline phase [29].

A decrease in activity at W/Mo ratios higher than about $(2.6\text{--}5.1) \times 10^{-4}$, observed in Fig. 2, is believed to be due to the coverage of the catalyst active sites, which are responsible for the conversion of propane to propylene in Path I (known as the RDS of propane oxidation), with the excessive amounts of the added W species.

4.4. Selectivity for acrylic acid

Fig. 3 indicated that the selectivity for acrylic acid changed with the amounts of added WO_x, showing a maximum at the W/Mo ratios of 1.3×10^{-4} to 1.3×10^{-3} , which was a trend similar to the one observed for the conversions of propane (Fig. 2). The similar trend in the dependence of the selectivity and the activity of the catalysts on the W loading suggests that the two parameters were affected by a common factor that was modified by the W addition. It is believed that the promotion of the dehydration step on the W-added catalysts was responsible for the characteristic changes of the two parameters.

The propane conversions increased when the dehydration step in the RDS was promoted, as discussed above. The selectivity was determined by the relative rates of individual steps in Paths I and III, instead of Path II that proceeded at low rates. The promotion of Path I by the W addition, due to the increased rates of dehydration in the RDS, likely contributed to the increased selectivity. The selectivity was also affected by the relative rates of the dehydration and the dehydrogenation of 2-propanol in Path III. Because the added W species promoted the dehydration step to greater extents than the dehydrogenation step, as discussed above (Section 4.2), selectivity was improved by the W addition.

The selectivity would be lowered by the additional steps that converted propylene to either 2-propanol or acetone (Fig. 10), which are known to be promoted on the acidic sites of the catalysts [12,15]. Acidic sites are also detrimental to selectivity because they promote the complete oxidation of products. However, the results of NH₃-TPD (Fig. 7) indicated that the W addition decreased the amounts of acidic sites in the catalyst, thus contributing to an increase in the selectivity. Based on the above arguments, it can be concluded that the selectivity was improved on the W-added catalysts, because the dehydration step was promoted to a greater

extent than the dehydrogenation step, and because the amounts of the acidic sites were decreased.

5. Conclusions

The WO_x-modified catalysts showed higher activity for the partial oxidation of propane compared with the unmodified catalyst (Mo_{1.0}V_{0.3}Te_{0.23}Nb_{0.23}O_x), because the amorphous WO_x promoted the steps involved in the RDS of propane oxidation: the partial oxidation of propane to oxygenates and the dehydration of the oxygenates to propylene. The enhanced oxygen mobility in the W-added catalyst also contributed to propane oxidation.

The added WO_x species also improved acrylic-acid selectivity, because the species promoted the dehydration of propanols, which were produced as the intermediates of propane oxidation, and additionally decreased the amounts of acidic sites in the catalyst to suppress side reactions leading to undesired oxygenate products.

Acknowledgements

This work was supported by Brain Korea 21 (BK 21) project, National Research Laboratory (NRL) program, LG Chemical Co., and the Center for Ultramicrochemical Process Systems (CUPS).

References

- [1] M.M. Lin, Appl. Catal. A 207 (2001) 1–16.
- [2] M. Ai, T. Ikawa, J. Catal. 40 (1994) 203–211.
- [3] T. Ushikubo, H. Nakamura, Y. Koyasu, S. Wajiki, US Patent 5,380,933 (1995).
- [4] R.K. Grasselli, Catal. Today 49 (1999) 141–153.
- [5] E. Thorsteinson, T. Wilson, F. Young, P. Kasai, J. Catal. 52 (1978) 116–132.
- [6] T. Ohara, M. Ueshima, I. Yanagisawa, JP Patent 47-42241B (1972).
- [7] N. Kurata, T. Matsumoto, T. Ohara, K. Oda, JP Patent 42-9805B (1967).
- [8] I. Nagai, I. Yanagisawa, M. Ninomiya, T. Ohara, JP Patent 58-17172B (1983).
- [9] G. Blanchard, G. Ferre, EP Patent 609,122-A1 (1994).
- [10] C. Mazzocchia, E. Tempesti, R. Anouchinsky, A. Kaddouri, FR Patent 2,693,384 (1994).
- [11] M. Lin, M. Linsen, EP Patent 962,253,A2 (1999).
- [12] M. Baca, A. Picamo, J.L. Dubois, J.M.M. Millet, Catal. Commun. 62 (2005) 215–220.
- [13] M. Takahashi, S. To, S. Hirose, JP Patent 98,118,491 (1998).
- [14] M. Lin, T.B. Desai, F.W. Kaiser, P.D. Klugherz, Catal. Today 61 (2000) 223–229.
- [15] P. Concepción, P. Botella, J.M. López Nieto, Appl. Catal. A 278 (2004) 45–56.
- [16] B. Mitra, I.E. Wachs, G. Deo, J. Catal. 240 (2006) 151–159.
- [17] C.D. Baertsch, K.T. Komala, Y.-H. Chua, E. Iglesia, J. Catal. 205 (2002) 44–57.
- [18] D. Kulkarni, I.E. Wachs, Appl. Catal. A 237 (2002) 121–137.
- [19] M. Ai, J. Catal. 101 (1986) 389–395.
- [20] A. Kaddouria, C. Mazzocchia, E. Tempesti, Appl. Catal. A 180 (1999) 271–275.
- [21] L. Luo, J.A. Labinger, M.E. Davis, J. Catal. 200 (2001) 222–231.
- [22] J.M. Oliver, J.M. López Nieto, P. Botella, A. Mifsud, Appl. Catal. A 257 (2004) 67–76.
- [23] P. Botella, E. García-González, J.M. López Nieto, J.M. González-Calbet, Solid State Sci. 7 (2005) 507–519.
- [24] J.M. López Nieto, P. Botella, B. Solsona, J.M. Oliver, Catal. Today 81 (2003) 87–94.
- [25] M. Gotić, M. Ivanda, S. Popović, S. Musić, Mater. Sci. Eng. B 77 (2000) 193–201.
- [26] M. Deepa, M. Kar, S.A. Agnihotry, Thin Solid Films 468 (2004) 32–42.
- [27] W. Kuang, Y. Fan, Y. Chen, J. Colloid Interface Sci. 215 (1999) 364–369.
- [28] M. Alifanti, J. Kirchnerova, B. Delmon, D. Klvana, Appl. Catal. A 262 (2004) 167–176.
- [29] H. Hosono, J. Non-Cryst. Solids 352 (2006) 851–858.